

Induction Zone Length Measurements for Regular Cell Pattern by Nitric Oxide Planar Laser-Induced Fluorescence

M. Alicherif, K.P. Chatelain, S.B. Rojas Chavez, D.A. Lacoste

Mechanical Engineering Program, Physical Science and Engineering Division, King Abdullah University
... of Science and Technology (KAUST), Thuwal, 23955-6900, Saudi Arabia

Clean Combustion Research Center (CCRC), King Abdullah University of Science and
... Technology (KAUST), Thuwal 23955-6900, Saudi Arabia

1 Introduction

Detonation is the supersonic mode of propagation of combustion waves in premixed reactive mixtures. It is associated with high energy release, pressure, and temperature for short characteristic time and length scales. Thus, detonations are attractive for applications such as propulsion or power generation. Near Chapman-Jouguet velocity, detonations are characterized by a three-dimensional (3D) structure and are intrinsically unstable. The interactions of the transversal waves with the propagating front lead to an uneven release of energy producing the cell structure. It is an universal characteristic of gaseous detonations identified by Denisov and Troshin [1] and is a reliable indication of their properties. In particular, the mean cell width, corresponding to the mean width of the cells projected in a plan, is associated with the induction zone length of the exothermic reaction in the detonation front. The cell regularity, corresponding to the general regularity of the cell structure, is associated with the reactivity of the mixture and can be correlated with numerical parameters, such as the activation energy (θ) and the stability parameter (χ). Far from the limits of propagation these properties only depend on the thermodynamic conditions and the composition of the fresh gas and are essential to the understanding of the detonation phenomenon.

The most accessible technique to characterize the cell structure is the soot-foil, first developed by Shchelkin and Troshin [2], which provides information on the mean cell width and cell regularity from the interaction of the waves with the surface of the foil. The drawback of this technique is that it is time-integrated. Schlieren imaging was performed by Takai et al. [3] to obtain instantaneous information on a propagating front such as the temporal evolution of the shock within one cell cycle but the technique and results are sights integrated. To overcome this issue, more studies in narrow channels were performed by several groups [4–7] but the properties of such detonations are no longer independent of the confinement conditions. Recent works of Pintgen et al. [8], Mével et al. [9], and Rojas Chavez et al. [10] focused on the planar laser-induced fluorescence of hydroxyl radical (OH-PLIF) technique to obtain two dimensional (2D) time-resolved information on the reaction zone of the detonation front. To characterize the induction zone length Chatelain et al. [11] and Rojas Chavez et al. [12] performed one-dimensional (1D) laser induced-fluorescence of nitric oxide (NO-LIF). Recently, the 1D results

were confirmed in 2D by Rojas Chavez et al. [13] by conducting planar laser-induced fluorescence of nitric oxide (NO-PLIF) in two different hydrogen detonations. Their results showed a large range of measured induction zone lengths that could not be precisely correlated with the time of the cellular cycle. The present work is dedicated to the study of the evolution of the induction zone length within the cellular cycle by a combination of the soot-foil measurements and NO-PLIF for a stable H_2 detonation mixture.

2 Experimental Setup and Methods

The same experimental setup as in [14] was employed in this work, which is an updated version of the previous experimental setup employed in [11, 12]. The total length of the rig was increased to 3.5 m to allow Chapman-Jouguet (CJ) detonation for a wider variety of initial conditions. The visualization section was modified to keep a quartz window on one side and a soot foil holder on the facing wall. The side-wall soot foils were made of 350 mm-long, 120 mm-wide, and 1 mm-thick stainless steel plates and smoked with a thin carbon deposit. The dimensions of the plates were selected to obtain a large number of cells, between 6-20 cells in width and 50-80 cells in length, for the investigated initial conditions. The mixtures for this study were $2H_2:O_2:3.76Ar$ and $2H_2:O_2:3.76Ar$ seeded with 2000 ppm of NO at 20 kPa and 294 K.

The mean cell width and length were determined by a single observer measuring cells on at least three plates per condition to ensure reproducible and consistent results. Noises were avoided by eliminating all the dark spots, scratches, and random sub-structures from the selection, resulting in a total of 1890 cell width measurements for the two mixtures. It is important to note that, for the $2H_2:O_2:3.76Ar$ mixture at 20 kPa and 294 K presented in this work, the main source of noise was associated with poor quality of smoking of the plates. The argon dilution allows for excellent cell regularity according to the classification presented in [15] and the small addition of NO (2000 ppm), required for the NO-PLIF measurements, did not modify it [14]. The observed standard deviations (1σ) of the cell width distribution for the mixture was small, around 0.7 mm, and the cell size was, therefore, considered regular. The experimental cell widths were measured with digital tools allowing for an uncertainty below the standard deviation.

The experimental procedure remains unchanged from [11, 12]. The experimental procedure enables to achieve repeatable detonation conditions $D/D_{CJ} = 1.00 \pm 3\%$ and $\phi = 1.00 \pm 1\%$ for H_2 - O_2 -Ar mixtures, at $T_0 = 294$ K and $P_0 = 20$ kPa initial conditions.

3 Results and Discussion

The distributions of cell widths and soot foil samples are presented in Fig. 1 for the case of $2H_2:O_2:3.76Ar$ mixture at 20 kPa and 294 K with and without NO (2000 ppm) seeding. The distribution is expressed as the ratio of the number of cells within a width interval (N) over the total number of cells (N_T). The results were obtained for a large number of cells, over multiple soot foils, and can be considered statistically representative of the cell width distribution. For both cases, the cell width is varying from 5 mm to 8.5 mm and the distribution is centered. The weighted mean width is also the most probable width at around 18% of representation, the variation of the cell width can be approached by a normal distribution around this maximum. It can also be concluded that the associated width corresponds to the mean cell width λ . For the two mixtures, with and without NO, the cell structures shown in the soot-foil samples are similar with a regularity that can be qualified as excellent. The images are in agreement with the statistical results as the mean cell width obtained is the same for the two mixtures, $\lambda = 6.7$ mm, and the cell regularity, expressed by the standard deviation of the distribution is also the same, $\sigma = 0.7$ mm.

From this figure, it can be concluded that a small addition of NO to the mixture does not, quantitatively, affect the cell structure (i.e., mean cell width and cell regularity). Thus, the NO seeded mixture can be used to characterize $\text{H}_2\text{-O}_2\text{-Ar}$ mixtures with the NO-PLIF diagnostic, at $T_0 = 294\text{ K}$ and $P_0 = 20\text{ kPa}$ initial conditions. For the rest of the study, only the NO seeded results will be presented and discussed, assuming they correspond to the detonation properties of the unseeded mixture.

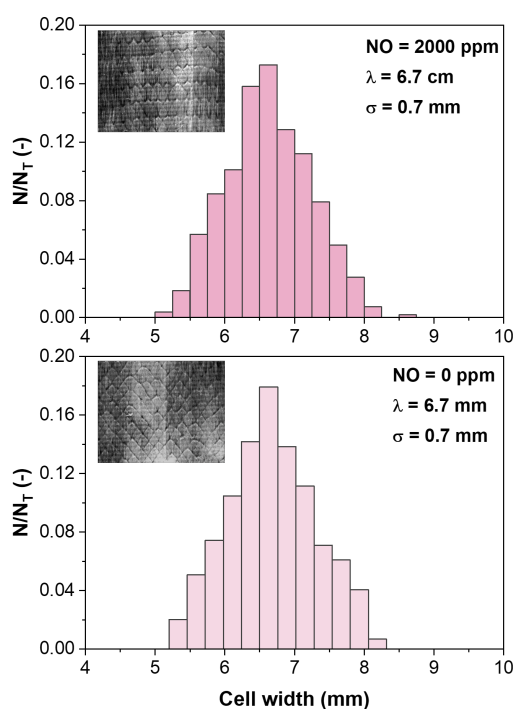


Figure 1: Soot foil samples and cell size distributions for $2\text{H}_2:\text{O}_2:3.76\text{Ar}$ with (top) and without (bottom) NO seeding at 20 kPa and 294 K initial conditions. N_T = total number of cells; N = number of cells associated with one width.

Figure 2 shows three single-shot NO-PLIF images obtained for three different shots. The detonation is propagating from left to right and we observe three characteristic zones in the pictures, namely the fresh gas, the induction zone and the burnt gases. The Fresh gas, on the right, at 20 kPa and 294 K initial conditions and small NO number density is emitting no/low LIF signal. The induction zone [12], that is intermediate, corresponds to conditions with elevated pressure and NO density and is emitting the highest LIF signal intensity with well-defined limits. The burnt gases, on the left, corresponds to conditions with elevated temperature from exothermic reactions and the resulting relatively low signal is a complex combination of NO LIF and OH^* chemiluminescence.

From these single-shot images, the instantaneous 2D structure of the propagating detonation front can be determined. In the shots 20-04 and 20-07, it is possible to identify the structure of 3 neighboring cells. For the two pictures, B represents one cell in the first half of its cycle where the front and the reaction zone are coupled inducing a thin induction zone. It is surrounded by two larger cells, A and C, in the second half of their cycles with a thicker local induction zone. In shot 21-05, it is possible to identify three characteristic steps of the cellular cycle. At the top, A' represents the smallest local induction zone associated with the shortest distance between triple points. This corresponds to the beginning of the cycle, right after the collision of two transversal waves. In the middle, B' is one of the greatest distances between triple points, which can be associated with a cell at the middle of its cycle and with a width

close or equal to λ . Finally, at the bottom, the front is slightly delayed compared to the top of the picture and we can observe the cell C' at the end of the cycle before the collision of the two transversal waves. The local induction zone length associated is one of the thickest that we recorded.

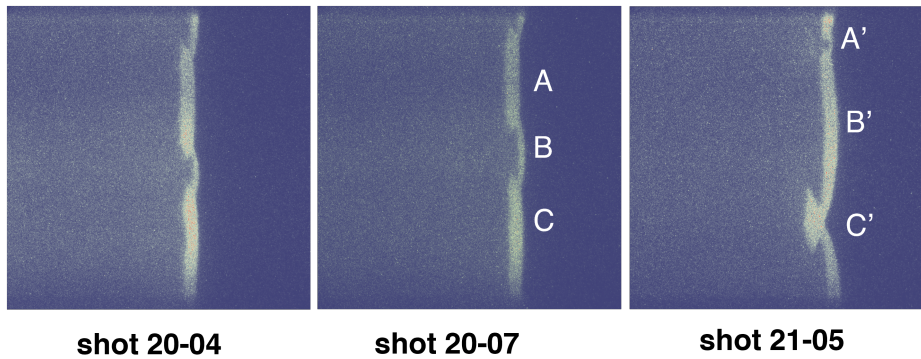


Figure 2: Examples of the detonation front visualizations obtained with the NO-PLIF technique for $2\text{H}_2:\text{O}_2:3.76\text{Ar-NO}(2000\text{ppm})$ mixture at 20 kPa and 294 K initial conditions.

Figure 3 displays qualitative profiles of the signal for the shot 21-05. These profiles demonstrate the thickening of the local induction zone throughout the cell cycle. It was assumed that, given the regularity of the mixture and the repeatability of the experiments, we could associate the local induction zone evolution with the distances between triple points. The NO-PLIF results were obtained simultaneously with soot-foils to extract more information such as the corresponding length for a given local cell width. An illustrative schematic of the different cell distances utilized for this work is presented in fig. 4-a.

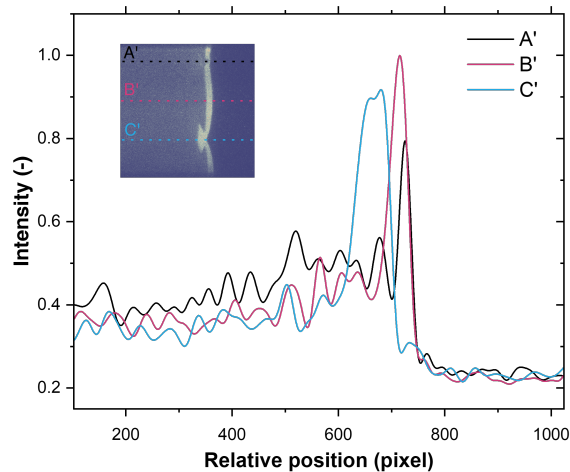


Figure 3: Qualitative profile of the fluorescence signal at different stages of the cell cycle obtained from shot 21-05. Each profile corresponds to a different cell.

Figures 4-b and -c present the reconstruction of the cell's local induction zone within one cycle. Figure 4-b is the variation of the local induction length with the local width (w). It can be seen that the local induction length is very slowly increasing with w until it reaches $w=\lambda$. For the second part of the cycle, the local induction length thickens faster and with greater absolute variability. The same results can be deduced from the evolution of the local induction length within one cell cycle displayed in fig. 4-c.

For the first half of the cell, the front is propagating rapidly and the value of the local induction length is rising very slowly. The slope of the curve changes around 1/2 of the cell when the speed is already decaying, and the value of $w=\lambda$ is reached around 2/3 of the cell cycle. From this value, we observe different slopes for the evolution of local induction zone length and great variability of the value for the same position. These results can be correlated with the fact that when the front starts to lose speed we observe a decoupling of the front with the reaction zone leading to a thickening of the local induction zone length. This decoupling seems to be associated with significant variability of the local induction zone length for the second half of the cell cycle. The numerically defined CJ induction length seems to agree with the local induction zone length recorded for the first half of the cell cycle.

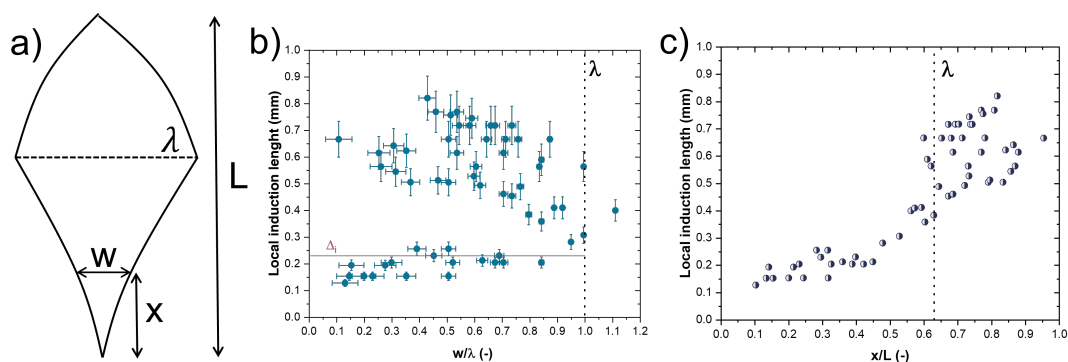


Figure 4: a) Schematic of a cell, the length (L) and width (λ) are obtained with soot foil; b) variation of the local induction length with the local width (w); c) reconstruction of the evolution of the local induction length within one cell cycle.

4 Conclusion

This work aimed at measuring the local induction zone length for a propagating detonation in a regular mixture using NO-PLIF and reconstructing its evolution by complementary soot foil measurements. This work was performed for a stable mixture, $2\text{H}_2:\text{O}_2:3.76\text{Ar}$ with NO (2000 ppm) seeding at 20 kPa and 294 K initial conditions, and the conclusions are:

- The cell regularity is excellent for the mixture with and without NO addition and the observed cell width is the same. It was assumed that the NO seeding had no impact on the dynamic parameters of the detonation and the NO-PLIF measurements are a reliable representation of the properties of the $2\text{H}_2:\text{O}_2:3.76\text{Ar}$ detonation at 20 kPa and 294 K initial conditions.
- The NO-PLIF images allow obtaining qualitative information about the 2D local induction zone that can be easily separated from the fresh gas and the burnt gases. The results are single shot and time-resolved. We observed a thickening of the induction zone length within the cellular cycle.
- With a combination of the soot foil experiment and the NO-PLIF measurements it is possible to reconstruct the evolution of the local induction zone length within one cell cycle. It was seen that the induction zone length thickens slightly in the first half of the cell cycle and greatly in the second half of the cell cycle. This change of slope is also associated with significant variability of the local induction zone length for the second half of the cycle.

The results constitute a first step in the understanding of the evolution of the local induction zone length by NO-PLIF and will be followed by more experiments in mixtures associated with fair and poor cellular structure.

References

- [1] Denisov, Yu N., Troshin, Y.K. (1959). Pulsating and spinning detonation of gaseous mixtures in tubes. Dokl. Akad. Nauk SSSR. Vol. 125.
- [2] Shchelkin, K.I., Troshin, Y.K. (1964). Gasdynamics of Combustion. English Translation NASA-TT-F-23.
- [3] Takai, R., Yoneda K., and Hikita T. (1975). Study of detonation wave structure. Symposium (International) on Combustion. Vol. 15. No. 1. Elsevier.
- [4] Nagaishi, T., Yoneda, K., and Hikita, T. (1971). On the structure of detonation waves in gases. Combustion and Flame, 16(1), 35-38.
- [5] Edwards, D. H., and RJ, M. (1972). Instabilities in the reaction zones of detonation waves.
- [6] Strehlow, R. A., and Crooker, A. J. (1974). The structure of marginal detonation waves. Acta Astronautica, 1(3-4), 303-315.
- [7] Radulescu, M. I., Sharpe, G. J., Lee, J. H. S., Kiyanda, C. B., Higgins, A. J., and Hanson, R. K. (2005). The ignition mechanism in irregular structure gaseous detonations. Proceedings of the Combustion Institute, 30(2), 1859-1867.
- [8] Pintgen, F., Eckett, C. A., Austin, J. M., and Shepherd, J. E. (2003). Direct observations of reaction zone structure in propagating detonations. Combustion and Flame, 133(3), 211-229.
- [9] Mével, R., Davidenko, D., Austin, J. M., Pintgen, F., and Shepherd, J. E. (2014). Application of a laser induced fluorescence model to the numerical simulation of detonation waves in hydrogen–oxygen–diluent mixtures. International Journal of Hydrogen Energy, 39(11), 6044-6060.
- [10] Chavez, S. B. R., Chatelain, K. P., Guiberti, T. F., Mével, R., and Lacoste, D. A. (2021). Effect of the excitation line on hydroxyl radical imaging by laser induced fluorescence in hydrogen detonations. Combustion and Flame, 229, 111399.
- [11] Chatelain, K. P., Chavez, S. B. R., Vargas, J., and Lacoste, D. A. (2022). Towards Laser-Induced Fluorescence of Nitric Oxide in Detonation.
- [12] Chavez, S. B. R., Chatelain, K. P., and Lacoste, D. A. (2022). Induction zone length measurements by laser-induced fluorescence of nitric oxide in hydrogen-air detonations. Proceedings of the Combustion Institute.
- [13] Chavez, S. B. R., Chatelain, K. P., and Lacoste, D. A. (2022). Induction zone length measurements by laser-induced fluorescence of nitric oxide in hydrogen-air detonations. Combustion and Flame. (*Under review*)
- [14] Chatelain, K. P., and Alicherif, M., and Chavez, S. B. R., and Lacoste, Deanna A. (2023). Nitric oxide sensitization of hydrogen detonations. AIAA Scitech 2023 Forum, National Harbor, Maryland (2023). (*Accepted*)
- [15] Libouton, J. C., Jacques, A., and Van Tiggelen, P. J. (1981). Cinétique, structure et entretien des ondes de détonation. In Actes du Colloque International Berthelot-Vieille-Mallard-Le Chatelier (Vol. 2, pp. 437-442).